ACS Catalysis

Research Article

pubs.acs.org/acscatalysis

Achiral Ruthenium Catalyst Encapsulated in Titanium Phosphonate Homochiral Peptide-Based Solids for Enantioselective Hydrogenation of Ketones to Secondary Alcohols

Anat Milo[†] and Ronny Neumann*

Department of Organic Chemistry, Weizmann Institute of Science, Rehovot 76100, Israel

Supporting Information

ABSTRACT: Asymmetric homogeneous catalysis is well established, but the design of new chiral catalysts and the optimization of an existing catalytic system are time- and manpower-exhausting processes. Desirable, heterogeneous, chiral analogues to facilitate catalyst recovery are relatively rare or function poorly. Here we further develop our strategy for facile adaptation of known reactions involving homogeneous achiral catalysts to those involving heterogeneous asymmetric catalysts by use of a homochiral solid scaffold and show the generality of this concept, from hydrolysis and oxidation reactions to hydrogenations. In this case, an inexpensive "off-the shelf" achiral hydrogenation catalyst, $Ru^{II}Cl_2(R_2PCH_2CH_2NH)_2$, R = Ph, *i*-Pr, or *t*-Bu, embedded within a homochiral matrix is an enantioselective, recyclable heterogeneous catalyst for ketone hydrogenation. The amorphous matrix consists of tripodal poly(phenylglycine) capped with phosphonate moieties and cross-linked with titanium oxide. Hydrogenation of acetophenone derivatives can proceed with high enantioselectivity (up to 95% ee), and catalyst recycling by filtration is very effective.

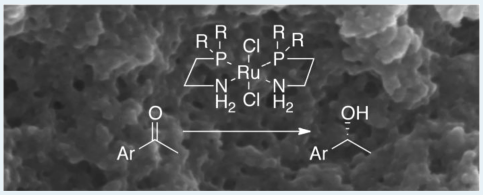

KEYWORDS: *heterogeneous catalysis, asymmetric catalysis, hydrogenation, ruthenium, reduction of ketones*

INTRODUCTION

The development of asymmetric homogeneous catalysts to elicit stereoselective transformations is an important branch of synthetic organic chemistry. In many cases, extensive optimization of chiral ligands and catalysts is required to achieve highly stereoselective reactions for specified substrates. Often, however, two major challenges remain. First, the discovery of catalytic systems for new asymmetric reactions and optimization of a catalytic system toward high stereoselectivity are time- and manpower-consuming efforts, which, although often effective, can yield homogeneous catalysts that are expensive and tend to be successful for a very limited reaction scope. Second, scaling up such catalytic reactions in a way that would be beneficial for industrial application requires an effective strategy for the recycling of catalysts. Heterogeneous catalysts hold practical advantages such as reduced contamination by catalyst residues leaching into the products, the safe and simple manipulation of workup, and the recovery and reuse of the costly chiral and metal resources. Several pathways have been taken toward this goal.[1−4] The most common method used is the immobilization of homogeneous asymmetric catalysts by adsorption onto surfaces, encapsulation within porous materials, or covalent tethering to inert matrixes,[1−7] yet such solutions typically yield significantly less active or stereoselective catalysts. Another approach is to modify surfaces with a chiral compound.[1−4,8] The successful use of platinum modified with a cinchona alkaloid for hydrogenation of pyruvate esters is a notable example.[9] More recently, incorporation of chiral ligands and/or catalysts into framework materials has become a hot topic with reported successes.[10−13]

We suggest that *readily available, "off the shelf", achiral catalysts* encapsulated in an insoluble, porous, homochiral scaffold could be a broad-spectrum approach toward a general and versatile method for stereoselective transformations. Toward this goal, a single homochiral platform could be used as a "reaction medium" for many transformations, which by variation of the catalyst could be used for oxidations, reductions, condensations, and so forth.

On the basis of research that has shown that tethers consisting of amide groups tend to self-organize through formation of intramolecular hydrogen bonds,[14] we have shown that homochiral polypeptides attached to a tripodal core capped with phosphonate moieties and cross-linked by condensation with titanium isopropoxide lead to an insoluble, porous, amorphous scaffold capable of hydrolyzing styrene oxide derivatives with very high enantioselectivity.[15] Incorporation of an achiral Mn−salen catalyst into this cross-linked peptidic phosphonate homochiral solid yielded an active catalyst for the epoxidation of styrene derivatives with low enantioselectivity (5−35% ee), but the intermediate epoxides were then hydrolyzed in situ on the support to yield the corresponding diols with very high enantioselectivity (>98%).[16] Now, we report the entrapment of an *achiral* hydrogenation

Received: August 29, 2012
Revised: October 14, 2012
Published: October 18, 2012

   dx.doi.org/10.1021/cs3005715 | ACS Catal. 2012, 2, 2531−2536

catalyst, $Ru^{II}Cl_2(R_2PCH_2CH_2NH)_2$, R = Ph, *i*-Pr, or *t*-Bu, within homochiral tripodal poly(phenylglycine) capped with phosphonate moieties and cross-linked with titanium oxide for the enantioselective hydrogenation of ketones to alcohols, with up to 95% ee being obtained in some cases. Furthermore, we show that for the studied reaction stable well-defined small mesopores (ca. 30 Å) lead to higher ee (%) values.

RESULTS AND DISCUSSION

The synthesis and characterization of the homochiral tripodal poly(phenylglycine) capped with phosphonate moieties (P-Phg) have been described in the past[15,16] and consist of the following steps: (1) polymerization of the *N*-carboxy anhydride (NCA) of L-phenyglycine on a tris(2-aminoethyl)amine (TAEA) initiator to yield a tripodal polymer with an average of 12 L-phenyglycine groups as determined by MALDI-TOF-MS analysis,[10−13] (2) amidation of the terminal amine moieties with $ClC(O)CH_2P(O)(OEt)_2$, and (3) mild hydrolysis of the phosphonate esters with Me_3SiBr to yield the tripodal polymer capped with phosphonic acid groups, P-Phg, Scheme 1.

Scheme 1. Illustrated Synthesis and Representation of the Ru-R/TiP-Phg Catalytic Assembly

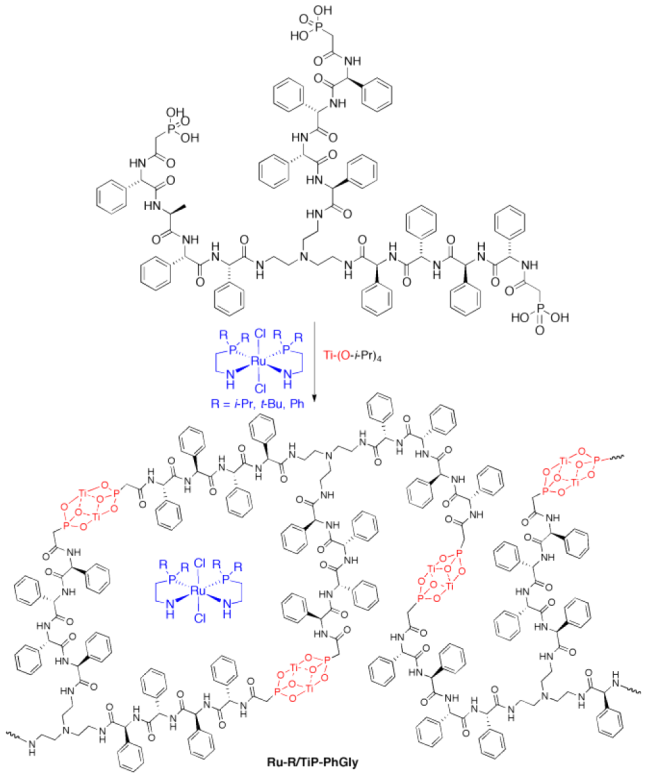

Polypeptides prepared by the NCA method tend to form strong intrachain (e.g., α-helix) and interchain (e.g., β-sheet) hydrogen bonds. In addition to hydrophobic, electrostatic, and dipolar interactions, these secondary structures contribute strongly to the self-assembly character of polypeptide chains. Most importantly, due to mild room temperature conditions and the nature of the reaction, NCA polymerization can afford peptides in both good yields and large quantities without detectable racemization at the chiral centers.[17−19]

The achiral catalyst $Ru^{II}Cl_2(R_2PCH_2CH_2NH)_2$ was incorporated into the homochiral polymer during a cross-linking procedure. The cross-linking procedure is based on the nonhydrolytic condensation of $Ti(O\text{-}i\text{-}Pr)_4$ with phosphonic acids, and slight variations of such procedures have been known to lead to assemblies with distinct morphologies.[20−23] Here, with P-Phg three variant cross-linking procedures were carried out. In the first case and similar to our previous reports,[15,16] P-Phg was reacted with $Ti(O\text{-}i\text{-}Pr)_4$ in DMSO and in the presence of $Ru^{II}Cl_2(R_2PCH_2CH_2NH)_2$ to yield Ru-R/Ti-Phg-1, for which, according to scanning electron microscopy−energy-dispersive spectrometry (SEM−EDS) analysis, the titanium:-phosphorus ratio was 4:3. In the second case a similar procedure was carried out, except, at the end of the nonhydrolytic condensation, water was added to complete the hydrolysis/cross-linking reaction to yield Ru-R/Ti-Phg-2 with a 4.25:3 titanium:phosphorus ratio. The third variant was also prepared by the two-stage procedure, however, using twice the amount of $Ti(O\text{-}i\text{-}Pr)_4$ to yield Ru-R/Ti-Phg-3, which was found to have a 3:1 titanium:phosphorus ratio. As will be shown, the various cross-linking procedures yielded assemblies with different surface areas and morphologies and showed different catalytic activities and stereoselectivities. The nitrogen sorption isotherms and Brunauer−Emmett−Teller (BET) plots for the three catalytic assemblies where $Ru^{II}Cl_2(Ph_2PCH_2CH_2NH)_2$, the most selective catalyst (see below), was incorporated into the homochiral scaffold are presented in Figure 1.

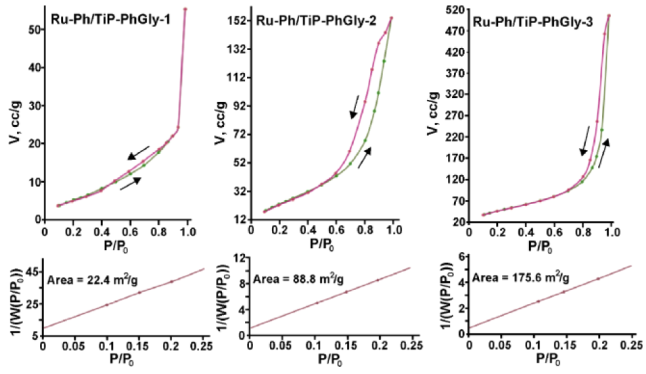

Figure 1. N_2 sorption isotherms (top) and BET plots (bottom) for Ru-Ph/TiP-Phg catalytic assemblies.

Assembly Ru-Ph/Ti-Phg-1 shows what appears to be a type III isotherm that is convex over its entire range and exhibits an indistinct B point (the first curvature of the isotherms). Such isotherms are associated with weak interactions between the material and the N_2 adsorbate; however, uncharacteristically for type III isotherms,[24−26] a slight hysteresis loop of type H4 appears at lower partial pressures that may be associated with swelling of a nonrigid porous structure. A rather low surface area of ~22 m^2/g was obtained for this material. When the initial nonaqueous condensation is followed by treatment with water to ostensibly complete the hydrolysis of the isopropoxide moiety of the $Ti(O\text{-}i\text{-}Pr)_4$ assemblies, the N_2 sorption is noticeably different, revealing type IV isotherms for Ru-Ph/Ti-Phg-2 and Ru-Ph/Ti-Phg-3.[24−26] The desorption isotherm distinctly follows a path different from that of the adsorption isotherm, resulting in a hysteresis, which in these two materials is confined to the multilayer region at high relative pressures. Hysteresis loops appearing in the multilayer range of physisorption isotherms are usually associated with capillary condensation in mesoporous structures. The surface areas for

dx.doi.org/10.1021/cs3005715 | ACS Catal. 2012, 2, 2531−2536

Ru-Ph/Ti-Phg-2 and Ru-Ph/Ti-Phg-3 were moderate to high, 89 and 176 m^2/g, respectively.

The standard Barrett–Joyner–Halenda (BJH) method for pore size distribution reveals a pore size of approximately 35 Å in all three materials. The average pore volumes were similar for Ru-Ph/Ti-Phg-2 and Ru-Ph/Ti-Phg-3 and higher for Ru-Ph/Ti-Phg-1 (see the Supporting Information, Figures S1–S3).[27] This pore size is in line with the XRD *d* spacing, Figure 2, and

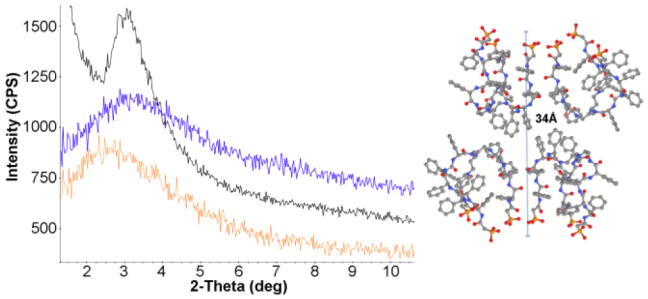

Figure 2. Powder XRD of Ru-Ph/Ti-Phg-1 (orange, *d* = 27.7), Ru-Ph/Ti-Phg-2 (black, *d* = 28.7), and Ru-Ph/Ti-Phg-3 (blue, *d* = 33.7). A model of the Ti-Phg scaffold is presented on the right.

our suggested model for intramolecular pores formed inside organic titanium phosphonate species.[10−14] For Ru-Ph/Ti-Phg-1 the pore size distribution is rather sharp, thus indicating that this is the most predominant pore size within this material. For Ph/Ti-Phg-2 there appears to be a slightly wider distribution of pore sizes with another peak at 88 Å, while Ru-Ph/Ti-Phg-3 exhibits a wide distribution of pore sizes with a peak at 177 Å. The Saito–Foley method,[28] generally developed for solids such as zeolites, was used for small mesopore analysis, leading to a pore size distribution with a maximum around 36 Å for Ru-Ph/Ti-Phg-1 and 32 Å for Ph/Ti-Phg-2 and Ru-Ph/Ti-Phg-3. These results may be inaccurate as this model assumes cylindrical micropores. They are, however, in the vicinity of what is expected according to XRD measurements, Figure 2, and the computational models previously constructed.[15,16]

Transmission and scanning electron micrographs of the three catalytic assemblies, Figure 3 and Figures S4 and S5,

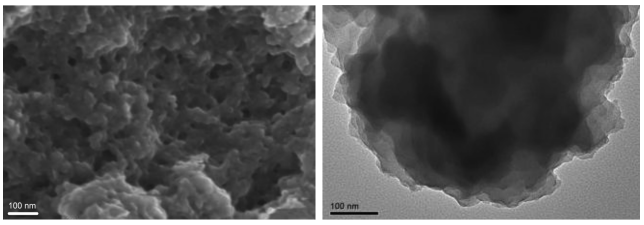

Figure 3. SEM (left) and TEM (right) images of Ru-Ph/Ti-PhGly-2.

Supporting Information, revealed a porous, yet well-organized and layered aspect for Ru-Ph/Ti-Phg-2 with a coral-like morphology. Ru-Ph/Ti-Phg-1, Figure S3, Supporting Information, also appeared ordered, yet the layers were less distinct, while Ru-Ph/Ti-Phg-3, Figure S4, is comprised of networked particles likely due to condensation and cross-linking of excess $Ti(O\text{-}i\text{-}Pr)_4$ in this assembly.

Initially, the catalytic efficacy was appraised for the hydrogenation of acetophenone as the substrate and various Ru-R/TiP-Phg-2 catalytic assemblies and for comparison also similar Ru-R/TiP-Leu-2 catalytic assemblies where L-leucine was used in place of L-phenyglycine on the homochiral scaffold, Table 1. This hydrogenation reaction typically requires base to

Table 1. Hydrogenation of Acetophenone Catalyzed by Ru-R/TiP-Phg-2 or Ru-R/TiP-Leu-2 (R = Ph, *i*-Pr, or *t*-Bu)[a]

catalyst	solvent	ee, %
Ru-*i*-Pr/TiP-Phg-2	buffer (pH 12.6)/THF (1:1)	33
Ru-*t*-Bu/TiP-Phg-2	buffer (pH 12.6)/THF (1:1)	58
Ru-Ph/TiP-Phg-2	buffer (pH 12.6)/THF (1:1)	70
Ru-Ph/TiP-Phg-2	buffer (pH 12.6)	55
Ru-Ph/TiP-Phg-2	buffer (pH 12.6)/THF (4:1)	53
Ru-Ph/TiP-Phg-2	buffer (pH 12.6)/diglyme (1:1)	52
Ru-*i*-Pr/TiP-Leu-2	buffer (pH 12.6)/THF (1:1)	28
Ru-*t*-Bu/TiP-Leu-2	buffer (pH 12.6)/THF (1:1)	36
Ru-Ph/TiP-Leu-2	buffer (pH 12.6)/THF (1:1)	40

[a]Reaction conditions: 0.1 mmol of acetophenone, 10 mg of catalyst, 1 mL of solvent, 2 atm of H_2, 60 h, 22 °C. (*R*)-1-Phenylethanol was the predominant product, and typically the yields were 20–25% with no observable byproducts. The ee was determined by HPLC using a Diacel OD-H column and 95:5 *n*-heptane/*i*-PrOH eluent. Note the heterogeneous catalyst asemblies are yellow-brown.

activate the catalyst,[29,30] and the preferred solvent was a phosphate buffer (pH 12.6)/THF (1:1) mixture. In a control reaction the scaffold alone, without an encapsulated ruthenium catalyst, under the same reaction conditions (Table 1) showed no hydrogenation. Also removal of the catalyst after 24 h stopped the reaction, indicating a true heterogeneous system. The phenyl-substituted achiral catalyst $Ru^{II}Cl_2(Ph_2PCH_2CH_2NH)_2$ gave the highest ee irrespective of whether the homochiral scaffold was L-phenylglycine or L-leucine based; the best catalyst was Ru-Ph/Ti-Phg-2, which showed the highest ee. The reactions showed a turnover frequency of about 1 per hour. The next step was to compare the variants of the Ru-Ph/TiP-Phg catalytic assemblies, Table 2.

As may be seen, the catalysts that were prepared by addition of water to complete the initial nonaqueous cross-linking Ru-Ph/TiP-Phg-2,3 and had showed type IV isotherms and seemingly mesoporous structures yielded consistently higher enantioselectivity for three substrates that were compared. Although Ru-Ph/TiP-Phg-3 has a notably higher surface area than Ru-Ph/TiP-Phg-2, the catalytic activity of the former was only slightly higher, and the enantioselectivity obtained was lower. The best catalyst, Ru-Ph/TiP-Phg-2, was also evaluated for additional substrates. Acetophenone derivatives with electron-donating substituents all showed quite high enantiomeric excesses, while electron-donating moieties reduced reactivity and the ee significantly. The larger 1-naphthylethanone was also much less reactive and yielded low enantioselectivity. The hydrogenation of ethyl pyruvate gave (*R*)-ethyl lactate with moderate enantioselectivity.

Since heterogeneous catalysis has the purported advantage of easy catalyst recovery, the recovery/recycling of the Ru-Ph/TiP-Phg-2 catalyst assembly was tested using acetophenone as the substrate over four catalytic cycles and by filtering the catalytic assembly, washing it with 2-propanol, and then drying it under vacuum. The yield of 1-phenylethanol was practically invariable, 20–21%, and the enantiomeric excess varied slightly, perhaps depending upon thoroughly drying the catalyst prior to reuse, 70%, 65%, 70% and 69% ee, respectively, for the four cycles.

dx.doi.org/10.1021/cs3005715 | *ACS Catal.* 2012, 2, 2531–2536

Table 2. Hydrogenation of Acetophenone Derivatives Catalyzed by Ru-Ph/TiP-Phg-1,2,3[a]

	Ru-Ph/TiP-Phg-2		Ru-Ph/TiP-Phg-1		Ru-Ph/TiP-Phg-3	
	yield, % (TON)	ee, %	yield, % (TON)	ee, %	yield, % (TON)	ee, %
C_6H_5COMe	20 (72)	70	20 (27)	26	30 (65)	65
4-$MeOC_6H_4COMe$	20 (42)	95	10 (12)	20	20 (34)	68
4-EtC_6H_4COMe	17 (48)	88	10 (12)	57	25 (42)	83
4-MeC_6H_4COMe	20 (42)	80				
4-ClC_6H_4COMe	3 (10)	12				
1-$COMeC_{10}H_7$	2 (6)	12				
ethyl pyruvate	20 (72)	46				

[a]TON = turnover number. Reaction conditions: 0.1 mmol of acetophenone, 10 mg of catalyst, 1 mL of phosphate buffer (pH 12.6)/THF (1:1), 2 atm of H_2, 60 h, 22 °C. The *R*-isomer was the predominant product with no observable byproducts. The ee was determined by using chiral HPLC columns, and the conversion was determined by gas chromatography with flame ionization detection (GC-FID) (see the Supporting Information for details). Each reaction was repeated at least three times, and an average was taken. The amount of Ru-Ph in each catalytic assembly was determined by EDS (27 μmol/g for Ru-Ph/TiP-Phg-2, 74 μmol/g for Ru-Ph/TiP-Phg-1, 58 μmol/g for Ru-Ph/TiP-Phg-3).

There remains the question of why the Ru-Ph/TiP-Phg-2 catalyst assembly gives the highest ee. Comparison of the FT-IR spectra of the catalytic assemblies, Figure 4, top, with that of

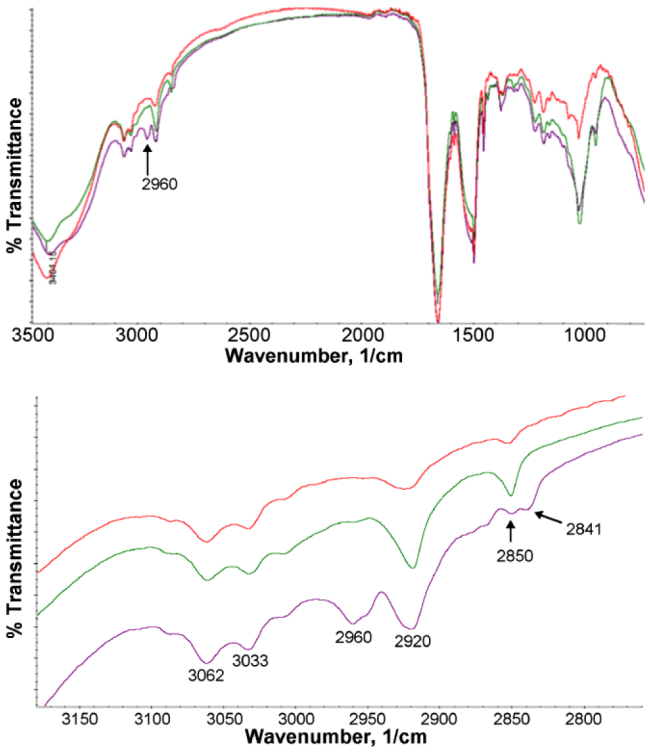

Figure 4. FT-IR spectra of Ru-Ph/Ti-Phg-1,2,3 (green, purple, and red, respectively).

the peptide-based scaffold, P-Phg, shows that P-Phg is not modified to a great extent during the condensation reaction and formation of the catalytic assembly. Furthermore, all three spectra show similar features. Some discrepancies can be found in the shift and intensity of the broad bands between 3000 and 3500 cm^{-1}, which are attributed to inter- and intramolecular stretching vibrations of hydrogen-bound nitrogen and oxygen. These discrepancies stem from hydration and variations to the extent of hydrogen bonding as a consequence of structural changes. In the range of 2800−3100 cm^{-1}, Figure 4, bottom, peaks at 2850 cm^{-1} are assigned to asymmetric CH_2 stretches and are associated with the phosphinoamino ligands of the encapsulated ruthenium catalyst since this peak is not observed in the phosphonate and phosphonic acid precursor. In the case of Ru-Ph/Ti-Phg-2, this peak is doubled, which may be attributed to a *Fermi resonance* possibly due to strong hydrogen bonding with an amide on the scaffold. The new peak at 2960 cm^{-1} is attributed to the stretch of the chiral CH on the scaffold, since it is the only CH moiety in this material. This peak appears much more strongly in Ru-Ph/Ti-Phg-2, likely due to a permanent dipole caused by strong hydrogen bonding. This peak can hardly be found in the spectra of Ru-Ph/Ti-Phg-1 and even less so in the spectra of Ru-Ph/Ti-Phg-3 and could indicate that the CH group in these two materials is not exposed to a permanent dipole moment.

The difference in molecular vibrations associated with the chiral CH group on the scaffold may explain the different stereoselective outcomes of catalytic reactions with these materials. Thus, in conjunction with the powder XRD, Figure 2, where the Ru-Ph/Ti-Phg-2 material showed the narrowest and sharpest peak indicative of higher structural order, one may conclude that there is a positive correlation between an ordered or defined pore network as indicated by the IR and XRD measurements and the ee observed in the catalytic reaction.

CONCLUSION

In this research three variants of encapsulated homochiral titanium phosphonates were prepared. All three materials consisted of a tripodal phenylglycine amino acid backbone and an encapsulated, commercially available, achiral ruthenium hydrogenation catalyst. Slight variations in the preparation procedure led to three materials with different surface areas, pore structures, and morphologies that were elicited in the yield and ee obtained in the hydrogenation reactions. Although the ruthenium catalyst is achiral, its encapsulation within a homochiral titanium phosphonate led to the reduction of ketones to secondary alcohols with various degrees of enantioselectivity (up to 95% ee). The exposure to water immediately after the nonhydrolytic condensation in the case of Ru-Ph/Ti-Phg-2 led to the stabilization of the titanium phosphonate layered structure and to a narrower distribution of chiral pores. These features, which can be seen in the electron microscopy images and are also evident from the N_2 sorption, IR, and XRD analyses, correlate with the higher ee values obtained using this material as a catalyst. Thus, careful design of chiral materials with well-defined pores has been introduced as a rational pathway for the formation of heterogeneous asymmetric catalysts. This study significantly supplements our previous research where homochiral titanium

dx.doi.org/10.1021/cs3005715 | *ACS Catal.* 2012, 2, 2531−2536

phosphonates based on tripodal amino acid scaffolds were introduced for hydrolysis and oxidation reactions. The generality of the concept is that chirality of a solid reaction medium can induce highly enantioselective transformations upon an encapsulated achiral catalyst through *remote effects*, that is, without ligation of a chiral ligand to the active site. It should be noted that remote effects have also been observed in homogeneous assemblies upon attaching catalysts to protein.[31] In addition, our group has also shown that remote effects are in play in aqueous biphasic media upon encapsulation of achiral catalysts into chiral poly(ethylenimines).[32] Interestingly, in this case phenylglycine derivatives gave better results than leucine derivatives, possibly because additional $\pi-\pi$ interactions between the aromatic ketone substrates and the catalyst scaffold may have an additional directing effect. Further optimization is still needed. For example, the turnover frequency is low relative to those of the homogeneous analogues, possibly due to diffusion limitations or less active catalyst entities. After optimization a scenario leading to applications of this concept in heterogeneous asymmetric catalysis could be envisioned.

EXPERIMENTAL PART

Synthesis of Ru-Ph/Ti-Phg-1. The tripodal pepetide P-Phg was prepared and characterized as previously described, and the molecular weight was calculated according to MALDI-TOF-MS analysis.[16] Ti(*i*-PrO)$_4$ (300 μL, 280 mg, 0.988 mmol) in 5 mL of anhydrous DMSO was added dropwise to a solution of P-Phg (0.5 g, ca. 0.236 mmol) and $Ru^{II}Cl_2(Ph_2PCH_2CH_2NH)_2$ (25 mg, 0.016 mmol) in 14 mL of anhydrous DMSO and the resulting solution vigorously stirred under an argon atmosphere in a sealed glass pressure tube for 72 h, during which a brown gel-like precipitate was formed. The gel was separated by centrifugation at 8000 rpm, then washed with water and diethyl ether, and dried under reduced pressure to afford 0.3 g of fine brown powder. Anal. Found: C, 45.35; H, 4.83; N, 7.04. TiO_x 9% (by TGA). $^{31}P\{^1H\}$ MAS NMR: δ = −2.17, 12.78.

Synthesis of Ru-Ph/Ti-Phg-2. Ti(*i*-PrO)$_4$ (300 μL, 280 mg, 0.988 mmol) in 5 mL of anhydrous DMSO was added dropwise to a solution of P-Phg (0.5 g, ca. 0.236 mmol) and $Ru^{II}Cl_2(Ph_2PCH_2CH_2NH)_2$ (25 mg, 0.016 mmol) in 14 mL of anhydrous DMSO and the resulting solution vigorously stirred under an argon atmosphere in a sealed glass pressure tube for 72 h, during which a brown gel-like precipitate was formed. The reaction mixture was added to 25 mL of deionized water and left for 2 h; the solid was separated by centrifugation at 8000 rpm, washed with water and diethyl ether, and dried under reduced pressure to afford 0.4 g of fine yellow-brown powder. Anal. Found: C, 45.08; H, 4.80; N, 6.18. TiO_x 18% (by TGA). $^{31}P\{^1H\}$ MAS NMR: δ = −2.63, 11.69. IR (KBr, ν, cm^{-1}): 500−700 (TiO vibrations), 698.5, 732.63 (monosubstituted benzene CH bend and ring puckering); 953.7, 1029.48 (titanium phosphonate P−O bend); 1102.6 (titanium phosphonate P−O stretch); 1223.5 (phosphonic acid C−P stretch); 1302, 1319.1 (amide N−H bend and C−N stretch); 1399.1 (CH_2 bend); 1586.0, 1603.6 (C=C aromatic stretch); 1454.6, 1497.3, 1507.5 (amide N−H bend and C−N stretch); 1657.2 (amide C−O stretch); 2850 (asymmetric CH_2 aliphatic stretch); 2920 (symmetric CH_2 aliphatic stretch); 2960 (aliphatic CH stretch); 3031.5, 3063.3 (aromatic ring stretch); 3298.5, 3395.2−3700 (amide N−H stretch and hydrogen-bound water and phosphonate).

Similar procedures were carried out for other achiral catalysts, $Ru^{II}Cl_2(R_2PCH_2CH_2NH)_2$, where R = Ph, *i*-Pr, and *t*-Bu, and for L-leucine-based scaffolds, P-Leu.

Synthesis of Ru-Ph/Ti-Phg-3. Ti(*i*-PrO)$_4$ (600 μL, 560 mg, 1.976 mmol) in 5 mL of anhydrous DMSO was added dropwise to a solution of P-Phg (0.5 g, *ca.* 0.236 mmol) and $Ru^{II}Cl_2(Ph_2PCH_2CH_2NH)_2$ (25 mg, 0.016 mmol) in 14 mL of anhydrous DMSO and the resulting solution vigorously stirred under an argon atmosphere in a sealed glass pressure tube for 72 h, during which a brown gel-like precipitate was formed. The reaction mixture was added to 25 mL of deionized water and left for 2 h; the solid was separated by centrifugation at 8000 rpm, washed with water and diethyl ether, and dried under reduced pressure to afford 0.5 g of fine yellow-brown powder. Anal. Found: C, 48.63; H, 4.77; N, 7.81. TiO_x 34% (by TGA). $^{31}P\{^1H\}$ MAS NMR: δ = −2.3, 12.51.

Catalytic Reactions and Analysis. A 10 mg mass of catalyst was added to a 20 mL glass pressure tube; 500 μL of THF (without stabilizer) was added, followed by the addition of 500 μL of phosphate buffer (pH 12.6, 0.15 M Na_3PO_4 and 0.03 M Na_2HPO_4). The pressure tube was purged with H_2 three times and then brought to 2 atm of H_2, and the contents were stirred for 2 h, after which 10 μL of substrate was added. The suspension was again purged three times, then brought to 2 atm of H_2, and left to react for 60 h at room temperature (~22 °C). The reaction mixtures were analyzed by GC to determine the conversion and yield. Only the ketone substrate and the alcohol product were observed. Enantiomeric excesses were measured using chiral HPLC columns as follows: 1-phenylethanol, Diacel OD-H, 95% heptane, 5% 2-propanol, 1.0 mL/min; 4-methoxy-1-phenylethanol, Diacel OD-H, 99% heptane, 1% 2-propanol, 1.2 mL/min; 4-methyl-1-phenyl-ethanol, Diacel OD, 99.5% heptane, 0.5% 2-propanol, 2.6 mL/min; 4-ethyl-1-phenylethanol, Diacel OD, 99.5% heptane, 0.5% 2-propanol, 2.6 mL/min; 4-chloro-1-phenylethanol, Diacel OD, 99% heptane, 1% 2-propanol, 2.5 mL/min; 1-naphthylethanol, Diacel OD-H, 90% heptane, 10% 2-propanol, 1.0 mL/min. The absolute configuration of the isomer in excess was determined as *R* for all substrates by optical rotation. The enantiomeric excess of (*R*)-ethyl lactate was measured using a chiral GC column (Lipodex-C, 25 m, 0.25 mm i.d.) using racemic ethyl lactate and (*S*)-ethyl lactate as reference compounds.

ASSOCIATED CONTENT

Supporting Information

Details on the experimental methods for the characterization of catalysts and their activity, N_2 sorption data, and electron micrographs. This material is available free of charge via the Internet at http://pubs.acs.org.

AUTHOR INFORMATION

Corresponding Author

*E-mail: Ronny.Neumann@weizmann.ac.il.

Present Address

[†]Department of Chemistry, University of Utah, Salt Lake City, UT.

Notes

The authors declare no competing financial interest.

■ ACKNOWLEDGMENTS

This research was supported by the Minerva Foundation and the Helen and Martin Kimmel Center for Molecular Design. R.N. is the Rebecca and Israel Sieff Professor of Organic Chemistry.

■ REFERENCES

(1) Heitbaum, M.; Glorius, F.; Escher, I. *Angew. Chem., Int. Ed.* **2006**, *45*, 4732−4762.
(2) De Vos, D. E.; Vankelecom, I. F. J.; Jacobs, P. A. *Chiral Catalyst Immobilization and Recycling*; Wiley-VCH: New York, 2000; pp 320.
(3) Bein, T. *Curr. Opin. Solid State Mater. Sci.* **1999**, *4*, 85−96.
(4) Ding, K., Uozumi, Y., Eds. *Handbook of Asymmetric Heterogeneous Catalysts*; Wiley-VCH: New York, 2008.
(5) McMorn, P.; Hutchings, G. J. *Chem. Soc. Rev.* **2004**, *33*, 108−122.
(6) Hutchings, G. J. *Annu. Rev. Mater. Res.* **2005**, *35*, 143−166.
(7) Corma, A.; Garcia, H. *Top. Catal.* **2008**, *48*, 8−31.
(8) Studer, M.; Blaser, H.-U.; Exner, C. *Adv. Synth. Catal.* **2003**, *345*, 45−65.
(9) Buergi, T.; Baiker, A. *Acc. Chem. Res.* **2004**, *37*, 909−917.
(10) Ding, K.; Wang, Z.; Wang, X.; Liang, Y.; Wang, X. *Chem.—Eur. J.* **2006**, *12*, 5188−5197.
(11) Wang, Z.; Chen, G.; Ding, K. *Chem. Rev.* **2009**, *109*, 322−359.
(12) Yoon, M.; Srirambalaji, R.; Kim, K. *Chem. Rev.* **2012**, *112*, 1196−1231.
(13) Lin, W. *Top. Catal.* **2010**, *53*, 869−875.
(14) Borovik, A. S. *Acc. Chem. Res.* **2005**, *38*, 54−61.
(15) Milo, A.; Neumann, R. *Adv. Synth. Catal.* **2010**, *352*, 2159−2165.
(16) Milo, A.; Neumann, R. *Chem. Commun.* **2011**, *47*, 2535−2537.
(17) Deming, T. J. *J. Polym. Sci., Part A: Polym. Chem.* **2000**, *38*, 3011−3018.
(18)) Cotarca, L.; Eckert, H. *Phosgenations—A Handbook*; Wiley-VCH: New York, 2003; pp 668.
(19) Katakai, R.; Iizuka, Y. *J. Org. Chem.* **1985**, *50*, 715−716.
(20) Vioux, A.; LeBideau, J.; Mutin, P. H.; Leclercq, D. *Top. Curr. Chem.* **2004**, *232*, 145−174.
(21) Mutin, P. H.; Guerrero, G.; Vioux, A. *C. R. Chim.* **2003**, *6*, 1153−1164.
(22) Guerrero, G.; Mutin, P. H.; Vioux, A. *Chem. Mater.* **2000**, *12*, 1268−1272.
(23) Villa-García, M. A.; Jaimez, E.; Bortun, A.; García, J. R.; Rodríguez, J. *J. Porous Mater.* **1995**, *2*, 85−89.
(24) Brunauer, S.; Deming, L. S.; Deming, W. S.; Teller, E. *J. Am. Chem. Soc.* **1940**, *62*, 1723−1732.
(25) Sing, K. S. W.; Everett, D. H.; Haul, R. A. W.; Moscou, L.; Pierotti, R. A.; Rouquerol, J.; Siemieniewska, T. *Pure Appl. Chem.* **1985**, *57*, 603−619.
(26) Rouquerol, J.; Avnir, D.; Fairbridge, C. W.; Everett, D. H.; Haynes, J. H.; Pernicone, N.; Ramsay, J. D. F.; Sing, K. S. W.; Unger, K. K. *Pure Appl. Chem.* **1994**, *66*, 1739−1758.
(27) Barrett, E. P.; Joyner, L. G.; Halenda, P. P. *J. Am. Chem. Soc.* **1951**, *73*, 373−380.
(28) Saito, A.; Foley, H. C. *AIChE J.* **1991**, *37*, 429−436.
(29) Noyori, R.; Ohkuma, T. *Angew. Chem., Int. Ed.* **2001**, *40*, 40−73.
(30) Noyori, R.; Kitamura, M.; Ohkuma, T. *Proc. Natl. Acad. Sci. U.S.A.* **2004**, *101*, 5356−5362.
(31) c.f. Ward, T. R. *Acc. Chem. Res.* **2011**, *44*, 47−57.
(32) Levi, N.; Neumann, R. ChemPlusChem. http://dx.doi.org/10.1002/cplu.201200203 (accessed August 31, 2012).